forests

MDPI

Article

Microbial Diversity and Ecosystem Functioning in Deadwood of Black Pine of a Temperate Forest

Roberta Pastorelli [1,*], Alessandro Paletto [2], Alessandro Elio Agnelli [1], Alessandra Lagomarsino [1] and Isabella De Meo [1]

[1] Research Centre for Agriculture and Environment, Consiglio per la Ricerca in Agricoltura e l'Analisi dell'Economia Agraria, I-50125 Firenze, Italy; alessandroelio.agnelli@crea.gov.it (A.E.A.); alessandra.lagomarsino@crea.gov.it (A.L.); isabella.demeo@crea.gov.it (I.D.M.)

[2] Research Centre for Forestry and Wood, Consiglio per la Ricerca in Agricoltura e l'Analisi dell'Economia Agraria, I-38123 Trento, Italy; alessandro.paletto@crea.gov.it

* Correspondence: roberta.pastorelli@crea.gov.it; Tel.: +39-055-2492247

Abstract: The present study provides a deeper insight on variations of microbial abundance and community composition concerning specific environmental parameters related to deadwood decay, focusing on a mesocosm experiment conducted with deadwood samples from black pine of different decay classes. The chemical properties and microbial communities of deadwood changed over time. The total carbon percentage remained constant in the first stage of decomposition, showing a significant increase in the last decay class. The percentage of total nitrogen and the abundances of *nifH* harbouring bacteria significantly increased as decomposition advanced, suggesting N wood-enrichment by microbial N immobilization and/or N_2-fixation. The pH slightly decreased during decomposition and significantly correlated with fungal abundance. CO_2 production was higher in the last decay class 5 and positively correlated with bacterial abundance. Production of CH_4 was registered in one sample of decay class 3, which correlates with the highest abundance of methanogenic archaea that probably belonged to *Methanobrevibacter* genus. N_2O consumption increased along decomposition progress, indicating a complete reduction of nitrate compounds to N_2 via denitrification, as proved by the highest *nosZ* gene copy number in decay class 5. Conversely, our results highlighted a low involvement of nitrifying communities in deadwood decomposition.

Keywords: logs; decay classes; microbial diversity; microbial abundance; functional microbial groups

Citation: Pastorelli, R.; Paletto, A.; Agnelli, A.E.; Lagomarsino, A.; De Meo, I. Microbial Diversity and Ecosystem Functioning in Deadwood of Black Pine of a Temperate Forest. *Forests* **2021**, *12*, 1418. https://doi.org/10.3390/f12101418

Academic Editor: Bartosz Adamczyk

Received: 8 September 2021
Accepted: 11 October 2021
Published: 18 October 2021

1. Introduction

Lying deadwood—the dead trees and debris on the forest floor—is a natural and fundamental structural and functional component of forest ecosystems. It influences biological, physical, and chemical processes [1], and plays a key role in biodiversity and soil fertility maintenance [2,3]. Indeed, lying deadwood provides important habitats and nourishment for several saproxylic species [4], being an essential substrate for numerous insects and fungi [5].

Deadwood decay level is a key variable affecting deadwood-inhabiting fungi, bryophyte presence and diversity, and the dynamics of carbon release and sequestration. Some studies highlighted that the richness of saproxylic species is highest in the first two decay classes of conifers and in the third decay class of broadleaves [6,7]. According to the deadwood classification system adopted in many national forest inventories (NFIs), five decay classes [8] were considered in this study: recently dead, weakly decayed, medium decayed, very decayed, and almost decomposed. This classification system also corresponds to the five-class system used in the Italian National Forest Inventory [9].

Deadwood biomass is one of the five terrestrial carbon (C) pools—together with above-ground and below-ground biomass, soil, and litter—that are relevant for estimation of C stocks and changes under the United Nation Framework Convention on Climate

Change (UNFCCC) and Kyoto Protocol [10]. During its decomposition, it undergoes significant transformations, thus being fundamental in C and nitrogen (N) redistribution to soil and atmosphere [11,12].

In traditional forest management—focused on the maximisation of timber production in time and space—standing dead tree and lying deadwood are removed during the silvicultural interventions because the accumulation of deadwood is considered a potential risk for forest fires and pollution [13], a potential source of pests and diseases [14], and an obstacle to recreational activities [15]. Conversely, in biodiversity-oriented forest management one of the aims is to reduce differences in deadwood volume between managed and natural forests, while in close-to-nature forest management deadwood is even considered a key functional and structural component of forests supporting habitats and species diversity [2,16].

Deadwood is a habitat for many specialised organisms, including microbes, invertebrates, bryophytes, lichens, and vascular plants [17]. Wood-inhabiting fungi and bacteria are the key decay agents, and from their perspective, deadwood represents both a habitat and a resource [18]. Saprophytic fungi, in particular Basidiomycota, produce arrays of extracellular enzymes and actively contribute to breaking down cellulose, hemicellulose, and lignin, supplying themselves with substrates for their growth [19]. Bacteria also have crucial decay abilities, but less attention has been paid to their specific roles in wood decay [20–24].

Fungi and bacteria may develop intricate relationships of synergic, antagonistic, and/or neutral nature [25], influencing wood decay rates and community functions [18]. Bacteria may benefit from products released by the fungal decomposition processes [20,26] and, on the other side, may provide N, iron, and growth factors to stimulate fungal growth and accelerate the rate of wood decay [27–29]. Both fungal and bacterial decay abilities are shaped by environmental conditions and biotic interactions [25] and the microbial community composition and function change as decomposition progresses [18].

Microorganisms play crucial roles in maintaining the equilibrium between organic matter decomposition, C sequestration, and greenhouse gas (GHG) exchanges from soil to atmosphere in forests [30]. The complex interactions between microbial decomposition activities and the atmosphere may therefore constrain or amplify climate change processes [30].

However, there is a poor understanding of the relationships between microbial diversity and deadwood decomposition at present. Thus, obtained information on microbial species or functional groups involved in decaying processes is of paramount importance for the prediction of the responses of forests to climate change [31], and new data are needed to help in elucidating the processes regulating GHG fluxes from deadwood.

The cultivation-independent molecular methods, generally including the direct extraction of total microbial DNA, have been the most common approaches to determine microbial diversity in various environments [32]. Among these, the polymerase chain reaction-denaturing gradient gel electrophoresis (PCR-DGGE) fingerprinting has already been used to provide indications on the relative changes in deadwood and litter microbial community composition as decomposition progressed [33–37]. The best approach to identify and quantify specific microbial groups and/or enzymes related to processes of the C and N cycles is to use real time PCR of marker genes of the respective microbial groups (e.g., 16S rDNA genes) or that encodes the process-related enzymes [38–40].

In this study we applied PCR-DGGE and real-time PCR to provide new insights into the changes in composition and function of the decomposer microbial communities in response to wood decay. Furthermore, we tested the hypothesis that microbial communities' abundance and composition are related to substrate quality (total C and N contents, C/N ratio) and potential GHG fluxes (carbon dioxide, CO_2; methane, CH_4; nitrous oxide, N_2O) at different stages of natural decay. To do so, a mesocosm experiment was set up with deadwood samples of different decay classes collected from black pine logs in a temperate forest ecosystem. We explored microbial communities (fungi, bacteria, and archaea) and specific functional communities linked to C and N cycles. Several marker genes were

used, including the 16S rRNA genes of methanogens archaea and CH_4-utilising bacteria (methanotrophs), in the C cycle. We quantified the genes: *nifH* (encoding dinitrogenase); *amoA* (encoding ammonia monooxygenase); *nirK* (encoding copper nitrite reductase); and *nosZ* (encoding nitrous oxide reductase), as suitable indicators to estimate N_2-fixation, nitrification, and denitrification potential, in the N cycle.

2. Materials and Methods

2.1. Experimental Design and Deadwood Sampling

The mesocosms consisted of deadwood cores of different decay classes placed into a 1 L Erlenmeyer flask closed with a silicone gas-tight cap and incubated at controlled moisture and temperature (see Section 2.2). The deadwood cores were collected from black pine (*Pinus nigra* J.F. Arnold) lying deadwood on April 2018, by using a battery drill (20.4 V) with a modified bit to provide a cylindrical core of 3 cm diameter. The deadwood cores were extracted from the middle of the log piece with the drill bit towards the ground, immediately placed in a sterile plastic bag, and then transported to laboratory for mesocosms set up.

A total of 20 deadwood cores were collected, in 18 circular fixed-area plots (13 m radius; 531 m^2) randomly located in the study area where field measurements for deadwood assessment and dendrometric data were realized [41]. Lying deadwood was subjectively selected in the different plots and distributed among five decay classes (four deadwood cores within each decay class) in accordance with a 5-decay class system [5,42]. The five decay classes were assigned by two technicians, working together, using a visual classification system considering the main visual characteristics of deadwood (Table S1) [8,43]. The selection of black pine lying deadwood was carried out in the Pratomagno massif, a mountain area that borders the Apennine ridge located in the north-east of the Tuscany region in Italy (43°27′ N; 9°11′ E). The average elevation is of 1150 m a.s.l., with a south-west exposure and 40% average slope. The geological substrate is characterized by quartz-feldspar sandstones alternated by siltstones and argillites [44]. Soils are generally moderately deep and very rich in organic matter in topsoil "A" horizon (average content 6.8%) [45]. The forest is spread over the temperate continental sub-Mediterranean bioclimatic zone [46] and is dominated by 57 years-old black pines plantations—Calabrian pine (*Pinus brutia* Ten. subsp. *brutia*) and Austrian black pine (*Pinus nigra* J.F. Arnold) [45]. The average annual temperature is 10.5 °C with maximum temperatures registered in July and minimum temperatures in January. The average annual precipitation amount is 997 mm with a maximum peak in autumn and minimum precipitation in June [44].

2.2. GHG Potential Production from Deadwood

The potential production of GHGs (CO_2, N_2O, CH_4) was estimated by measuring for 48 h the gas produced by each deadwood core within the mesocosm, as described by [33].

Briefly, the day after collection, each deadwood core was weighed and put into a 1 L Erlenmeyer flask closed with a silicone gas-tight cap and incubated at 20 °C. To keep the internal moisture constant during the test, a plastic tube containing 3 mL of water was added within each flask. Gas production was measured at the beginning of the experiment and after 6, 9, 24, and 48 h. At each incubation time, 25 mL headspace gas samples were collected with an air-tight 30 mL propylene syringe and immediately pressurized into a pre-evacuated 12 mL glass Exetainer® vials (Labco Ltd., Buckinghamshire, UK) with a septa screw cap (Labco Ltd., Buckinghamshire, UK). Concentrations of CO_2, N_2O, and CH_4 were analysed using a GC-2014 gas chromatograph (Shimadzu Corporation, Kyoto, Japan) with a thermal conductivity detector (TCD) for CO_2, a ^{63}Ni electron capture detector (EDC) for N_2O, and a flame ionization detector (FID) for CH_4. The difference between blank and samples was always higher than the instrumental detection limit [33]. Gas concentrations were converted to mass per volume units using the Ideal Gas Law and measuring air temperatures and volumes, then expressed in mg g^{-1} considering the headspace of each

flask and the weight of each deadwood sample. The cumulative curve was calculated for each gas by summing the concentrations at each incubation time.

2.3. Physical and Chemical Properties

Moisture was determined immediately after the GHG production assay by measuring fresh weight and dry weight after incubation at 50 °C for 48 h.

The dry deadwood cores were firstly coarsely ground in a cutting mill (Retsch SM 100, Haan, Germany), at rotor speed of 1500 rpm min^{-1}, until a final fineness of 0.5 mm. Deadwood pH was determined using a digital calibrated pH meter (Hanna-pH211, Padova, Italy) on aqueous extract after shaking 1 g of dried deadwood coarse sawdust in 10 mL of distilled water for 120 min and left to decant for 30 min. Successively, deadwood samples were homogenized with a cutting mill (Retsch SM 100), at rotor speed of 1500 rpm min^{-1}, until a final fineness of 0.25 mm. Ten to twenty milligrams of deadwood fine sawdust was weighed into Ag-foil capsules and the % of total N (TN) and total C (TC) was measured by dry combustion on a Thermo Flash 2000 NC soil analyser (Fisher Scientific, Waltham, MA, USA) equipped with a thermal conductivity detector.

2.4. DNA Extraction and DGGE Analysis

The genomic DNA was extracted from 0.20 g of each deadwood coarse sawdust by using the FAST DNA SPIN kit for soil (Biomedicals, Santa Ana, CA, USA) according to the manufacturer's guidelines. DNA was eluted in sterile water and its integrity was verified by agarose gel electrophoresis (0.8% w/v).

DGGE analysis was performed to estimate the diversity and genetic structure of fungal, bacterial, and actinobacterial communities by using specific primer pairs for the V7–V8 region of fungal 18S rRNA gene (EF390—GCFR1; [47]), the V6–V8 region of bacterial 16S rRNA gene (GC986f—UNI1401r; [48]), and the V2–V3 region of actinobacterial 16S rRNA gene (F243 –R513GC; [49]). Amplification and DGGE procedures were carried out as previously described [33]. Evaluation of band migration distance and intensity within each lane of the DGGEs was performed using Gel Compare II software v. 4.6 (Applied Maths, Saint-Martens-Latem, Belgium). The number of bands and their relative abundance were used as a proxy of dominant taxon richness [50] and diversity (Shannon index) within each DGGE profile [51].

2.5. Real-Time PCR

Real-time PCR was carried out in a MJ Research PTC-200™ Chromo4 thermocycler (Bio-Rad Laboratories, Hertfordshire, UK) as described by [34]. The primer pairs used for the various microbial groups and functional genes were reported in Table S2. All samples were run in triplicate and negative control and standard curve were run in each plate. Data outputs were released by Opticon Monitor software (version 2.03 MJ Research).

For absolute quantification, the standard curves were created using plasmids containing target gene fragments amplified from reference strains or environmental samples (Table S2). The target gene PCR products were purified using PureLink™Quick PCR Purification kit (Invitrogen-Life Technologies, Carlsbad, CA, USA) and cloned using the pGEM-T Easy Vector System (Promega, Madison, WI, USA) according to the manufacturer's instructions. Approximately four clones from each target gene were randomly chosen and sequenced (BMR Genomics, Padova, Italy). The web-based BLAST tool available at the NCBI website (http://www.ncbi.nlm.nih.gov; accessed on 15 December 2020) was used to check specificity. Plasmid DNA was extracted using the QIAprep®Spin Miniprep kit (Qiagen, Hilden, Germany) and plasmid concentrations were determined by spectrophotometry using a BioPhotometer (Eppendorf, Hamburg, Germany). Standard curves were freshly prepared with 10-fold dilutions ranging from 3×10^8 to 3×10^2 gene copies μL^{-1}. The abundance of microorganisms in deadwood samples was expressed as gene copy number per gram of deadwood dry weight.

16S rRNA gene fragments obtained from DNA extracted from deadwood core number 12 (the one showing high CH_4 production) using methanogenic archaea primer set (Table S2) were also cloned. Twenty clones were randomly chosen and sequenced (BMR Genomics). The nucleotide sequences were aligned with each other using ClustaX 2.0.11 software and close related nucleotide sequences were determined comparing against all sequences stored in the GenBank database using the BLAST tool. Given the complete identity of the obtained sequences, only one sequence was deposited in the GenBank database under accession number MW412770.

2.6. Statistical Analyses

To assess the significant differences in relation to the decay class in deadwood physico-chemical properties, GHG cumulative emissions and microbial richness, and Shannon index, data were analysed by one-way analysis of variance (ANOVA) followed by Fisher least-significant difference (LSD) *post-hoc* test ($p < 0.05$) using Statistica 7 software (StatSoft, Palo Alto, CA, USA). The normality and the variance homogeneity of the data were tested prior to ANOVA.

Pearson correlation analysis was performed among deadwood physico-chemical properties (TC, TN, C/N, moisture, and pH), maximum values of GHGs (CO_2, CH_4, and N_2O) production, and total abundance of microbial groups by PAST3_21 software [52].

The banding patterns of each DGGE extracted as band-intensity matching tables were normalised by calculating the relative intensity of each band (ratio of the intensity of each band divided by the sum of the intensities of all bands in the same lane) and imported into PAST3_21 for multivariate statistical analysis. Non-metric multidimensional scaling (nMDS) was used to visualize differences of each DGGE profile in a two-dimensional space. One-way analysis of similarity (ANOSIM) and permutational analysis of variance (PERMANOVA) followed by pairwise comparisons were conducted to determine the extent of differences in microbial communities among decay classes. nMDS, ANOSIM, and PERMANOVA were performed using the Bray–Curtis distance measure and 9999 permutational tests; the accuracy of the nMDS plots was determined by calculating a 2D stress value.

Finally, the correlations between the fungal, bacterial and actinobacterial communities, deadwood properties, and CO_2 flux were determined by CCA performed with PAST3_21. DGGE bands were used as "species" data (filled symbols), while deadwood chemical properties (TN, TC, C/N, and pH) and CO_2 flux as "environmental" variables (vectors); the statistical significance was assessed using 999 permutational tests.

3. Results

3.1. Chemical Characterisation of Deadwood Samples

The results of moisture, TN and TC contents, C/N ratio, and pH were averaged according to the different decay classes and are reported in Table 1. The middle decay classes 2 and 3 showed the statistically significant lowest and highest values of relative moisture percentages, respectively. No significant differences were observed in the remaining classes.

The TN values significantly increased from decay class 1 to decay class 5 (Table 1), following an exponential trend ($R^2 = 0.93$). The middle decay classes (from 2 to 4) did not show statistically significant differences in TN content, whereas samples of the early decay class 1 and the late decay class 5 showed the significant lowest (0.18%) and highest (0.55%) values, respectively.

The TC percentage did not show a clear trend with the progression of deadwood decay. In the first three decay classes, the percentage of TC showed a stable trend setting on values of about 48%. A slight but not significant increase was observed in decay class 4, while the significant highest value was registered in decay class 5 (Table 1). Conversely, the C/N ratio followed a linear downward trend ($R^2 = 0.99$) from averaged 281.3 of decay class 1 to 102.7 of decay class 5.

The pH showed the highest values in the two early decay classes and the lowest values in the middle and late decay classes, respectively. Nevertheless, non-significant differences were found among decay classes (Table 1).

3.2. GHG Potential Production from Deadwood

Cumulative values of CO_2 potential production significantly increased over the advancement of deadwood decay, reaching the maximum from deadwood cores of the last decay class 5 (Figure 1a; Table S3). This increase followed a linear trend (R^2 = 0.99) from decay class 1 to decay class 5, except for the decay class 2, which showed a drastic drop in CO_2 production.

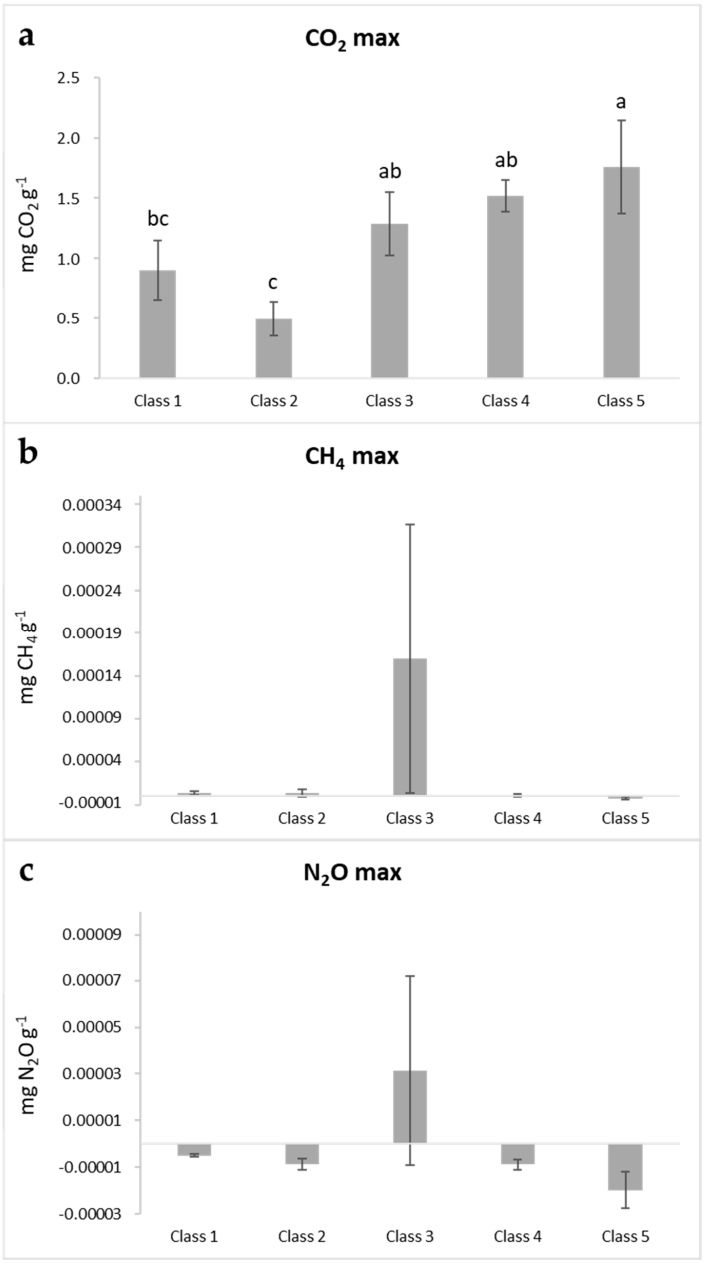

Figure 1. Maximum values of CO_2 (**a**); CH_4 (**b**); and N_2O (**c**) production from the black pine deadwood cores of the different decay classes. Error bars are the standard errors of four replicates. Different letters indicate significant differences at $p < 0.05$ among means.

The analysis of CH_4 and N_2O fluxes showed trends of both production and consumption, although no significant differences were observed among decay classes. The

average values of CH_4 potential production were low for decay classes 1, 2, and 4. Decay class 5 showed a negative averaged value (Figure 1b). Decay class 3 showed the highest value of CH_4 potential production, which is mainly due to a deadwood core (the number 12; Figure S1; Table S3) showing a production value (6.3×10^{-4} mg CH_4 g^{-1}) about 145 times higher than the averaged CH_4 potential production of all the other deadwood cores (4.3×10^{-6} mg CH_4 g^{-1}).

The N_2O potential production showed negative values in almost all deadwood cores, indicating mainly consumption of N_2O rather than production (Figure S2; Table S3). An exception was found in a deadwood core of decay class 3 (the number 9), which showed N_2O production (1.5×10^{-4} mg N_2O g^{-1}). The N_2O consumption showed an increasing trend from decay class 1 to decay class 5. However, all differences were not statistically significant (Figure 1c).

3.3. Structural Diversity of Deadwood Microbial Communities

Differences in the number and intensity of bands and band position along the DGGE profiles were revealed, depending on the decay class (Table 2, Figure S3). Overall, bacteria showed higher values of both richness and Shannon index compared to fungi. In both these microbial groups, the significant highest values of the two indices were found in the late decay class 5.

Actinobacteria showed decreasing values of richness and Shannon index from decay class 1 to decay class 5 (Table 2).

The nMDS ordinations of each DGGE showed profiles of decay class 1 clearly separated from those of the other decay classes (Figure 2). Fungal communities showed profiles of the early decay classes 1 and 2 distinctly grouped on the left side of the nMDS plot (Figure 2a). Replicates of decay classes from 3 to 5 exhibited a slight overlapping and showed a broad grouping positioned in the middle and on the right side of the *y*-axis. The stress value > 0.3 provides a weakly reliable representation of fungal similarity/dissimilarity in the nMDS graphical representation; thus, DGGE profiles were further analysed by multivariate analysis (see below).

Table 1. Average values of moisture, total C (TC) and total N (TN) contents, C/N ratio, and pH of the black pine deadwood cores from the different decay classes. Moisture, TC, and TN contents were calculated as percentage of the total dry mass of deadwood. Standard errors in parentheses. Different letters in a column indicate significant differences at $p < 0.05$ (LSD test) among means.

	Moisture (%)	TN (%)	TC (%)	C/N Ratio	pH
Class 1	52.2 (2.5) ab	0.18 (0.02) c	48.5 (0.4) b	281.3 (28.7) a	4.5 (0.3)
Class 2	41.7 (4.7) b	0.21 (0.03) bc	48.3 (0.8) b	240.0 (32.9) ab	4.6 (0.3)
Class 3	63.3 (3.0) a	0.27 (0.03) bc	48.4 (1.0) b	184.8 (19.9) bc	4.0 (0.1)
Class 4	54.6 (3.4) ab	0.31 (0.01) b	49.1 (0.5) b	158.0 (6.3) cd	4.1 (0.1)
Class 5	51.5 (10.6) ab	0.55 (0.08) a	52.2 (1.3) a	102.7 (18.7) d	4.0 (0.1)

Table 2. Average Richness and Shannon index calculated on 18S rDNA-DGGE band profiles from fungal community and on 16S rDNA-DGGE band profiles from bacterial and actinobacterial communities in decaying black pine deadwood, on the basis of decay class. Standard error in parentheses. Different letters in a column indicate significant differences at $p < 0.05$ (LSD test) among means.

	Fungi (18S-DGGE)		Bacteria (16S-DGGE)		Actinobacteria (16S-DGGE)	
	Richness	Shannon	Richness	Shannon	Richness	Shannon
Class 1	18.8 (1.3) b	2.86 (0.07) abc	15.0 (1.5) c	2.63 (0.12) c	11.0 (2.2) ab	2.29 (0.24) ab
Class 2	15.5 (0.9) b	2.67 (0.07) c	24.0 (2.9) b	3.09 (0.11) b	13.0 (2.0) a	2.51 (0.16) a
Class 3	18.5 (1.2) b	2.84 (0.07) bc	21.3 (0.8) b	2.99 (0.03) b	14.5 (0.6) a	2.66 (0.05) a
Class 4	22.8 (1.0) a	3.05 (0.05) a	26.0 (1.3) ab	3.17 (0.05) ab	6.8 (0.5) c	1.89 (0.07) b
Class 5	22.3 (1.2) a	3.01 (0.06) ab	29.8 (0.9) a	3.34 (0.03) a	7.5 (0.5) bc	2.00 (0.06) b
F	7.0	5.7	11.5	11.6	5.9	5.8
p	**	**	***	***	**	**

** $p < 0.01$; *** $p < 0.001$.

The bacterial nMDS ordination (Figure 2b) showed three distinct groups: the first comprising profiles of decay class 1, the second those of decay class 2, and the third those of decay classes 3, 4, and 5. The DGGE profiles of the intermediate and late stages of decomposition (decay classes 3–5) exhibited a high similarity (symbols are close); on the contrary, the DGGE profiles of the earlier stage (decay class 1) exhibited the greatest inter-specific variation (large distance among symbols).

Three broad groups could be highlighted in the actinobacterial nMDS graphical representation (Figure 2c). The profiles of decay class 1 formed a loose group on the left side of the *y*-axis; in the middle, it is possible to distinguish a group comprising the profiles of decay classes 2 and 3; on the right side of the plot were distinctly grouped profiles of decay classes 4 and 5. As for bacteria, the DGGE profiles of early (decay class 1) and late (decay classes 4 and 5) stages of decomposition showed the highest and lowest inter-specific variation, respectively.

Both bacterial and actinobacterial stress values (0.21 and 0.20, respectively) reflected a good representation of the observed distance among DGGE profiles.

Overall, the outcomes of ANOSIM and PERMANOVA global tests (Table S4) indicated a significant effect of decomposition stages on microbial community compositions ($p < 0.001$). The R values of the ANOSIM global test ranged from 0.54 to 0.66, confirming the consideration evinced by nMDS ordinations since, as a rule of thumb, $0.5 < R < 0.75$ was read as separate but overlapping communities [53]. Pairwise comparisons reinforced the nMDS remarks. Regarding fungal communities (Table S5a), the DGGE profiles of decay classes 1 and 2 were significantly different from each other and those of the other decay classes. DGGE profiles of class 3 were significantly different from those of decay class 5 but not from decay class 4. No significant differences were found between DGGE profiles of decay class 4 and those of decay class 5.

Bacterial communities showed statistically significant differences in DGGE profiles among each decay class (Table S5b). The lowest separation occurred between decay classes 3 and 5 and between decay classes 4 and 5 (R = 0.56 and 0.32, respectively). Actinobacterial communities showed significant differences among each decay class except between decay class 2 and decay class 3 and between decay class 4 and decay class 5 (Table S5c).

3.4. Quantification of Deadwood Microbial Communities

The state of decomposition differently affected the size of the different microbial groups inhabiting deadwood. Fungal 18S rRNA gene copies per gram of dry deadwood did not significantly differ between decay classes (Table 3). Bacteria were more abundant than fungi in each decay class. The number of bacterial 16S rRNA gene copies number significantly increased as the decomposition progressed, reaching the maximum value in decay class 5 (Table 3). A similar trend was observed for actinobacteria, although they showed nearly 10-fold lower values than bacteria (Table 3). In each of these three microbial groups, decay class 2 showed the lowest 16S rRNA gene copies number.

In addition, absolute quantification of CH_4-producing/-consuming microbial groups and functional genes linked to N-cycle was performed. The abundance of archaeal methanogens in deadwood was very low, of the order of 10^4–10^5 16S rRNA gene copies per gram of dry deadwood (Table 3). The highest values were observed in decay classes 3 and 5. The replicates of decay class 3 showed a high internal variation, thus there were no statistically significant differences in the averaged values compared to the other decay classes. By inspecting the abundance of methanogens of each deadwood core, the sample with the highest number of archaeal 16S rRNA gene copies per gram of dry deadwood corresponds to the core with the highest CH_4 production (core number 12; Figure S1). Sequencing of cloned PCR products from this deadwood core revealed the greatest nucleotide-sequence identity with *Methanobrevibacter* sp. (99.4% similarity to GenBank accession number AB026926 isolated from the gut of the termite *Hodotermopsis sjoestedti*).

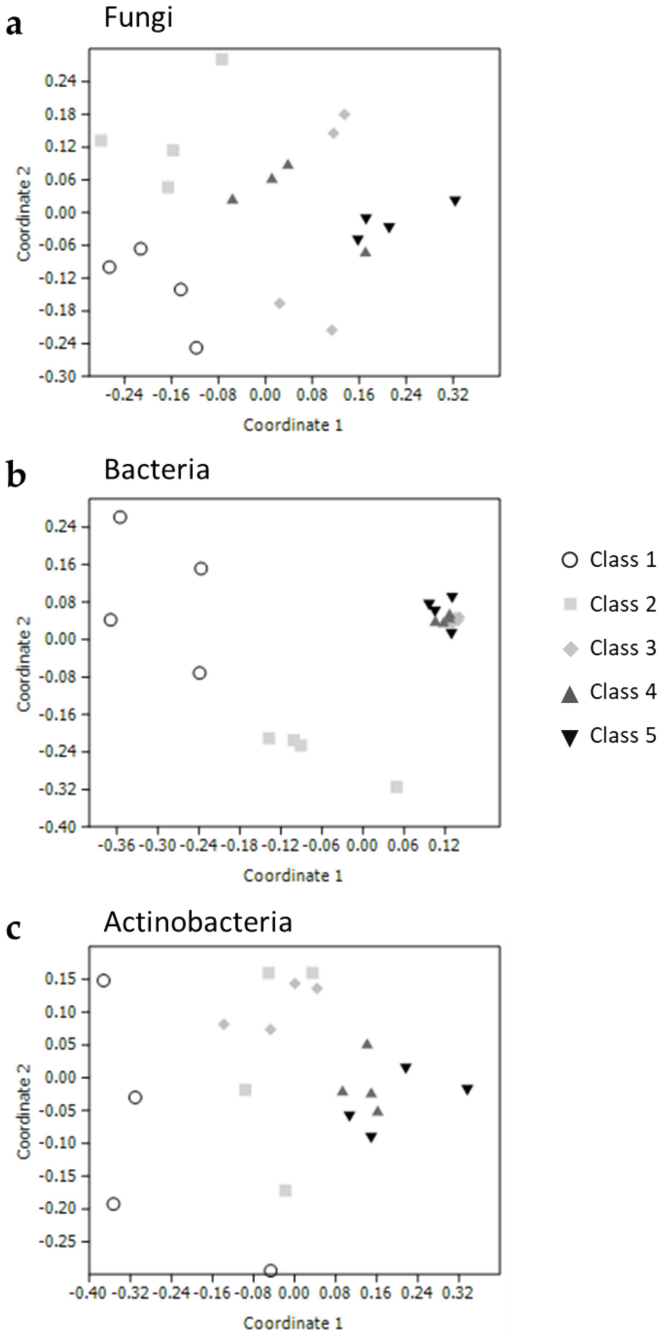

Figure 2. nMDS ordination plots of fungal 18S rDNA gene (**a**); bacterial 16S rDNA gene (**b**); and actinobacterial 16S rDNA gene (**c**) obtained by PCR-DGGE of extracted DNA from the black pine deadwood cores of the different decay classes.

The quantification of CH_4-consuming bacteria showed that methanotroph type I (group including the genera *Methylomonas* and *Methylobacter*) dominated the early decay class 1 (Table 3). In contrast, the methanotroph type II (group including the genera *Methylosinus* and *Methylocystis*) resulted as significantly more abundant in decay class 5 than in the less degraded classes (Table 3).

Overall, functional genes involved in processes of the N-cycle (N_2-fixation, nitrification, and denitrification) showed the highest values by a significant amount in decay class 5, which is generally 10-fold higher than other decay classes (Table 3). The abundance of the *nif*H gene varies from a minimum of 1.66×10^8 gene copies gr^{-1} dry deadwood of decay class 2 to a maximum of 4.18×10^9 gene copies gr^{-1} dry deadwood of decay

class 5. In each decay class, the archaeal *amo*A gene was more abundant than its bacterial counterpart (Table 3). In both ammonia-oxidising groups, the lowest values were found in decay class 2 and the highest values in decay class 5. The abundances of the two genes involved in the denitrification pathway, *nir*K and *nos*Z genes, did not differ much from one another in each decay class, reaching the maximum values in decay class 5 (Table 3).

Table 3. Real time PCR results for quantification of the various microbial groups in DNA extracted from the black pine deadwood cores of the different decay classes. Values are means with standard error in parentheses. Different letters in a row indicate significant difference at $p < 0.05$ (LSD test).

Microbial Group (*Target Gene*)	*n*. Copies gr^{-1} Deadwood				
	Class 1	**Class 2**	**Class 3**	**Class 4**	**Class 5**
Fungi (*18S rRNA*)	9.7×10^8 (8.7×10^8)	7.9×10^7 (2.2×10^7)	2.9×10^8 (1.7×10^8)	2.7×10^8 (1.4×10^8)	3.7×10^8 (2.6×10^8)
Bacteria (*16S rRNA*)	5.4×10^9 (1.6×10^9) b	5.4×10^8 (1.5×10^8) b	2.4×10^9 (3.7×10^8) b	2.6×10^9 (5.5×10^8) b	3.0×10^{10} (5.9×10^9) a
Actinobacteria (*16S rRNA*)	9.3×10^7 (3.3×10^7) b	7.8×10^7 (3.3×10^7) b	1.3×10^8 (3.6×10^7) b	2.0×10^8 (4.8×10^7) b	3.9×10^9 (6.7×10^8) a
Methanogens (*16S rRNA*)	1.6×10^5 (3.4×10^4) b	5.8×10^4 (9.0×10^3) b	4.7×10^5 (3.5×10^5) ab	4.2×10^4 (6.9×10^3) b	6.5×10^5 (9.1×10^4) a
Methanotrophs type I (*16S rRNA*)	1.1×10^9 (4.5×10^8) a	3.9×10^7 (1.9×10^7) b	3.5×10^7 (7.2×10^6) b	2.4×10^7 (1.0×10^7) b	6.5×10^7 (1.1×10^7) b
Methanotrophs type II (*16S rRNA*)	2.6×10^6 (2.1×10^6) b	2.9×10^6 (1.6×10^6) b	1.2×10^7 (6.5×10^6) b	4.5×10^6 (1.8×10^6) b	8.6×10^7 (4.9×10^7) a
Diazothrophs (*nifH*)	5.2×10^8 (2.9×10^8) b	1.7×10^8 (7.0×10^7) b	3.2×10^8 (1.3×10^8) b	3.3×10^8 (2.1×10^8) b	4.2×10^9 (1.2×10^9) a
Nitrifiers archaea (*amoA*)	5.8×10^5 (1.5×10^5) b	2.9×10^5 (2.8×10^4) b	5.6×10^5 (1.2×10^5) b	4.5×10^5 (5.9×10^4) b	4.7×10^6 (7.0×10^5) a
Nitrifiers bacteria (*amoA*)	3.8×10^5 (1.2×10^5) b	6.4×10^4 (1.9×10^4) b	2.1×10^5 (1.7×10^4) b	1.8×10^5 (4.6×10^4) b	2.0×10^6 (3.0×10^5) a
Denitrifiers (*nirK*)	2.5×10^7 (1.8×10^7) b	4.8×10^6 (3.5×10^6) b	7.7×10^6 (2.7×10^6) b	7.9×10^6 (1.3×10^6) b	1.6×10^8 (7.2×10^7) a
Denitrifiers (*nosZ*)	1.2×10^7 (4.7×10^6) b	4.6×10^6 (1.5×10^6) b	1.1×10^7 (4.1×10^6) b	1.4×10^7 (3.8×10^6) b	2.2×10^8 (3.3×10^7) a

3.5. Correlation Analysis

Significant ($p < 0.05$) Pearson's correlation coefficients between deadwood chemical characteristics, GHG fluxes, and abundances of inhabiting microbial groups were reported in Table 4. Fungi were negatively correlated to pH. Bacteria and actinobacteria were positively correlated to TN, TC, and CO_2 fluxes from deadwood and negatively correlated to C/N. The archaeal methanogens were positively correlated to CH_4 fluxes. Methanotrophs were positively correlated to pH (type I) and TN and TC (type II), whereas both types were correlated to C/N but in different directions (Table 4). The abundances of ammonia oxidisers were positively correlated to TC and TN and negatively to C/N. The diazotrophic bacteria were positively correlated to TN and TC. Finally, denitrifying bacteria-harbouring *nir*K gene were correlated only to TC content, whereas those harbouring the *nos*Z gene were positively correlated to TN and TC content and negatively to C/N.

Table 4. Pearson's correlation matrix of deadwood chemical parameters (TN, TC, C/N, and pH), maximum values of GHGs (CO_2, CH_4, and N_2O) production, and the microbial group abundances measures in deadwood cores from the different decay classes. Only significant Pearson correlation coefficients (r-values) are reported.

	TN	**TC**	**C/N**	**pH**	**CO_2**	**CH_4**	**N_2O**
CO_2	0.76 ***	n.s.	−0.80 ***	−0.62 ***	-	n.s.	n.s.
Fungi	n.s.	n.s.	n.s.	−0.48 *	n.s.	n.s.	n.s.
Bacteria	0.82 ***	0.54 *	−0.57 **	n.s.	0.60 **	n.s.	n.s.
Actinobacteria	0.83 ***	0.57 *	−0.61 **	n.s.	0.59 **	n.s.	n.s.
Methanogens	n.s.	n.s.	n.s.	n.s.	n.s.	0.75 *	n.s.
Methanotrophs I	n.s.	n.s.	0.44 *	0.54 *	n.s.	n.s.	n.s.
Methanotrophs II	0.55 *	0.65 **	−0.44 *	n.s.	n.s.	n.s.	n.s.
AOB	0.67 **	0.84 ***	−0.52 *	n.s.	n.s.	n.s.	n.s.
AOA	0.74 **	0.77 ***	−0.57 ***	n.s.	n.s.	n.s.	n.s.
nirK	n.s.	0.86 ***	n.s.	n.s.	n.s.	n.s.	n.s.
nosZ	0.72 **	0.75 **	−0.56 **	n.s.	0.46 *	n.s.	n.s.
nifH	0.46 *	0.78 **	n.s.	n.s.	n.s.	n.s.	n.s.

* $p < 0.05$; ** $p < 0.01$; *** $p < 0.001$.

The canonical correspondence analysis (CCA) showed the potential connections between changes in chemical characteristics, CO_2 production, and microbial community composition due to deadwood decay status (Figure 3). The linear species-environment

correlations along the first two axes accounted for more than 65% of explained variance and were significant ($p < 0.05$). A general shift of the microbial communities was observed from decay classes 1 and 2, on the right side of the CCA plot, to decay classes 4 and 5, on the left side of the CCA plot, passing through decay class 3, near the axes' intersection. The first two decay classes were mainly correlated to the C/N ratio and pH and presented the highest interspecific variation. On the contrary, the more degraded decay classes 4 and 5 resulted in being mainly correlated with TN, TC, and CO_2 production, and revealed the highest similarity. The distribution of species scores in the ordination diagram revealed that actinobacterial and bacterial taxa (light grey and grey dots, respectively) mainly contributed to separating the early decay classes from the late decay classes.

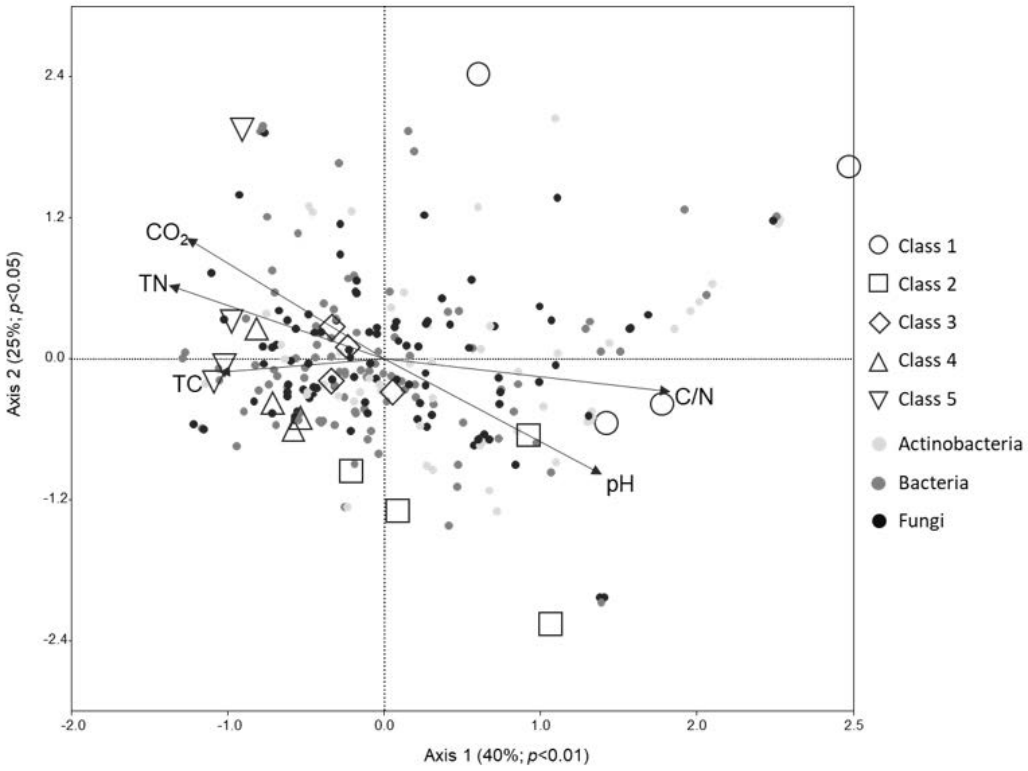

Figure 3. Canonical correspondence analysis (CCA) ordination diagram of microbial communities and environmental variables defined by the first and second axes. The percentage of variation in the data and significance is reported at each axis. The plots were generated by actinobacterial 16S rDNA gene (light grey dots), bacterial 16S rDNA gene (grey dots), and 18S rDNA gene (dark grey dots) DGGE banding patterns. Vectors represent deadwood pH; deadwood total C content (TC); deadwood total N content (TN); deadwood C/N ratio; and CO_2 flux from deadwood cores.

4. Discussion

4.1. Chemical Features of Deadwood Decay

In the first three decay classes, the percentage of TC content in deadwood cores remained constantly around 48%. After that, in late decay class 5, it showed a significant increase. Other studies conducted on temperate forests in Central Europe reported values of around 50% for individual tree species and, in particular, for conifers; the percentage of TC content is estimated to range from 48.0% to 52.1% [54]. Generally, the percentage of C content of deadwood remains stable during the whole decomposition process [55], although changes may occur following modifications in size and chemical composition, including lignin content.

Deadwood represents a significant proportion of forest C stock, accounting for 10–20% of the total C pool in mature forests [56]. Nevertheless, this C pool is transient because through the transformations operated by saprotrophic microorganisms, it is mainly released

into the atmosphere as CO_2, and the rest is sequestered in soil or within living biomass [29]. In our laboratory experiment, the CO_2 evolution from deadwood significantly increased in the late decay classes, leading us to assume that the activity of the microorganisms inhabiting deadwood increased along with decay progression, given the more favourable growth conditions created by the breakdown of structural biomolecules and the consequent release of nutrients. Thus, the increment of TC content in the decay class 5 should be due to C immobilization into microbial biomass because of the intensification of microbial growth and metabolic processes. According to this hypothesis, we observed bacteria as significantly more abundant in decay class 5 than in previous decay classes.

In our laboratory experiment, we observed lower CO_2 fluxes compared to another experiment conducted on deadwood cores collected from a comparable black pine forest in Monte Morello in the Tuscany region [33], although a consistent trend was shown.

Low values of TN content were observed in the early decay class 1, in agreement with fresh deadwood of most temperate and boreal trees that showed N content ranging between 0.03% and 0.18% of the dry mass [57]. Successively, the percentage of TN content experienced a slight and progressive increment till reaching more than twice the initial values in the decay class 5. Progressive N enhancement is a well-documented phenomenon in both conifers and broadleaf deadwood [33,34,58,59]. It depends on the synthesis of new N-rich compounds (i.e., proteins and nucleic acids) in actively growing microorganisms inhabiting deadwood, soil translocation mediated by ectomycorrhizal hyphae [29], and bacterial fixation of atmospheric N_2 [28].

Since N is often a limiting nutrient for the growth of microorganisms, its accumulation in deadwood represents a potentially high impact input for the microbial community. Accordingly, we found deadwood TN content positively and significatively correlated with CO_2 fluxes, indicating its importance as a driver of microbial activity.

As a simple consequence of increasing N concentration, the C/N ratio decreases during the advance of decomposition. The decrease of C/N ratio is a rough indicator of organic matter decomposability, supporting the evidence of different decomposition rates among decay classes, which are constrained by the availability of macronutrients [56].

The pH slightly decreases during decomposition. Wood pH was considered one of the main factors explaining significant differences in wood-inhabiting fungal community composition [60] since it is crucial for the functioning of extracellular fungal oxidoreductase. Generally, coniferous wood shows lower pH values than broadleaf, which may be due to stronger acidification by brown-rot fungi that prefer this type of wood [61,62]. What's more, the study area showed a soil pH similar to the wood pH registered in decay classes 1 and 2 [63], leading us to suppose that soil brown-rot fungi may have early colonized the deadwood logs, thus contributing to lowering the deadwood pH. Consistently with our results, Hoppe et al. [64] did not observe an important impact of pH in bacterial communities of deadwood.

4.2. Microbial Features of Deadwood Decay

Deadwood appeared to be rich in microbial biomass. Fungal abundance showed a marked decrease in the early stages of decomposition, although not significant. Successively, the number of fungi remained quite unchanged. Various studies have shown that bacterial, fungal, and archaeal density is minimal in fresh wood, increasing as the decomposition process advances [22,30]. In agreement, bacteria reached the highest value in decay class 5. On the other hand, bacteria dominated the microbial community in each decay class, showing counts that were generally one order higher than those of fungi, contrasting with results obtained by Tláskal et al. [29].

Fungi are the primary producers of enzymes that attack deadwood structural biopolymers [29]. Thus, fungi promptly intervene in the early stages of decomposition, playing a crucial role in opening the way in the physically recalcitrant substrate for colonization by other deadwood-inhabiting microorganisms. Tláskal et al. [29] found that more than 91% of transcripts of carbohydrate-active-enzymes decomposing biopolymers were of fungal

origin, whereas only 7% were assigned to bacteria. The actinobacteria phylum has been commonly found in bacterial communities colonizing deadwood [65] due to their excellent capabilities in degrading structural biopolymers, such as hemicellulose and cellulose [26]. In addition, they are presumably involved also in lignin degradation [66], although their role is still unclear. The size of actinobacterial community increased as decomposition progressed, although remaining one order lower than those of total bacteria. However, actinobacteria proved to be a noticeable representative group within the bacteria-inhabiting deadwood, reaching about 11% of the total bacteria in decay class 5. Overall, our results suggested that the decay processes gradually changed the deadwood logs composition, creating an environment more hospitable to both fungal and bacterial communities, in agreement with other authors [67].

We observed an increasing number of bacterial and fungal dominant taxa with the advancement of wood decay, as indicated by the significant increasing richness and Shannon index values. Our findings give reason to what was postulated by Gómez-Brandón et al. [68], that, as decomposition progresses, a higher number of ecological niches for microbial colonization become available, along with an increase in the wood's surface area and nutrient variety. In addition, our results suggested that increased metabolic diversity is required within bacterial and fungal communities to utilize the substrates that gradually become available as wood decays. Conversely, the deadwood actinobacterial community showed significantly lower species diversity in the late decay classes 4 and 5 compared to early decay classes. Thus, the actinobacterial community revealed a greater involvement in the degradation of more labile wood structural compounds, as hemicellulose and cellulose, in the early and intermediate phases of decomposition. Accordingly, Lynd et al. [69] postulated that actinobacteria are the most common initial colonizers of deadwood, and together with other pioneer bacterial groups, they contribute to increasing the permeability and the moisture uptake of wood, thus favouring fungal colonization [65]. Successively, an increased metabolic specialization was supposed for actinobacteria as an indication that the ability of lignin breakdown is limitedly spread within this microbial group [21].

The robustness of multivariate analyses results highlighted differences in microbial community composition of the five decay classes, suggesting the development of a succession of inhabiting microbial taxa with different metabolic activities, which reflects the gradual changes occurring in logs chemical properties during natural decay, as postulated by numerous authors [12,33,34,60,70].

4.3. GHG Emissions and Microbial Functional Groups

The CO_2 fluxes from deadwood cores were positively correlated with the increment in bacterial and actinobacterial 16S rRNA gene copy numbers. Although we are aware that gas fluxes registered into our lab-closed systems are not fully comparable to natural processes, this finding reinforces the assumption that the significant increase of bacterial biomass with increasing decay classes is consistent with the intensification of bacterial metabolic activities due to the increasing availability of substrates.

Deadwood represents an extensive and dynamic C stock of forest, playing fundamental roles as both source and sink of C. Its decomposition, together with forest fire, is one of the major inputs of CO_2 release from the earth surface with possible implications for global temperature increase [61]. In addition, also the potential evolution of CH_4 from deadwood has more considerable relevance in climate changes [71,72]. In a field mesocosm experiment conducted on black pine, Lagomarsino et al. [37] showed that deadwood was a substantial source of CO_2 and CH_4 in the atmosphere.

CH_4 production is primarily the result of archaeal-mediated wood material decomposition [71]. In addition, also brown-rot fungi are identified to produce CH_4 under anaerobic conditions [73]. We revealed the presence of methanogenic archaea in our deadwood logs, although they represented a tiny part of the prokaryotic community. The colonization of living tree tissue by methanogenic archaea was documented as early as the 1970s [67,74–77]. The highest value of 16S rRNA copy number was registered in a

deadwood core of decay class 3, accordingly with the highest production of CH_4. In this deadwood core, *Methanobrevibacter* was supposed to be the hypothetical CH_4 producer. It is assumed that the evolution of CH_4 mainly occurs as the result of symbiotic interactions between methanogenic archaea and xylophagous insects or wood-inhabiting protists and fungi [75,78,79]. Fungi cleave wood structural biopolymers and the products formed are fermented to produce CO_2 and H_2, which are substrates for the synthesis of CH_4 by methanogenic archaea [75]. Similarly, protists' endosymbiont methanogens may convert CO_2 produced by protists into CH_4 [80]. *Methanobrevibacter* was a strictly anaerobic prokaryote generally found to be associated with protists as symbiont or attached to the gut epithelium of both lower and higher termites [79]. In addition, *Methanobrevibacter* was also found in high abundance inside cells of *Spirotrichonympha leidyi*, a parabasalid flagellate that lives in termites' gut [79]. These findings lead us to hypothesize that the CH_4 production registered in our deadwood core was due to a symbiont association between prokaryotes and protists or fungi, whereas we did not find any evidence of termites or other xylophagous insects.

Except for one deadwood core, the CH_4 production showed a decline as decomposition progressed till reaching the highest negative values (CH_4 consumption) in decay class 5. Accordingly, Covey et al. [71] assumed that CH_4 emissions were highest in early decay stages because methanogenesis activity was fuelled by non-structural labile carbon substrates, and more abundant in early phases. An intensification of CH_4 oxidation in the late stage of decomposition may also be more advantageous for microorganisms than using recalcitrant structural compounds. In fact, CH_4 emitted from decaying wood may serve as a source of C and energy for aerobic CH_4-oxidizing (methanotrophic) bacteria [64,73,81]. We found that the methanotrophic bacteria represented a relatively high portion of the bacterial community of deadwood. The general increase of the CH_4 consumption with increasing decay class might suggest a relative higher involvement of this microbial group as decomposition progressed.

Methanotrophic bacteria can utilize also reduced C substrates with no C-C bonds, such as methanol, a by-product of fungal lignin decomposition [29,73]. Vorob'ev et al. [82] isolated methylotrophic microorganisms from beech wood blocks incubated on an acid forest soil surface during wood decay by the white-rot fungus *Hypholoma fasciculare*. Mäkipää et al. [83] found methanotrophs as core members of the diazotroph community in decaying Norway spruce logs. Therefore, it might be supposed that synergistic interactions between methanotrophs and fungi occur with the former providing N in return for methanol produced by the latter [84].

There is ever increasing evidence about the occurrence of inter-kingdom mutualistic interactions and their importance as drivers of ecosystem functioning related to nutrient cycling [85]. Bacteria are thought to play a marginal role in wood decomposition in contrast to their critical role in N wood-enrichment by N_2-fixation [68]. The amount of fixed N_2 during deadwood decomposition represents an important source of N entering the soil environment at the end of the deadwood life cycle [29]. N is a limited resource in wood; thus, fungi may meet their N requirements for vegetative growth and propagation through associations with diazotrophs [60,68]. In agreement, Hoppe et al. [64] reported a positive correlation between the number of fungal fruiting bodies and the diversity of the *nifH* gene in Norway spruce and European beech. Conversely, we did not find any significant correlation between fungi and *nifH* gene copies number.

The *nifH* gene copies number significantly increased with decay class, supporting the hypothesis of the increasing relevance of the role of the diazotrophic community as decomposition progresses. Using a metatranscriptomic approach in analysing the microbiome associated with decomposition of European beech, Tláskal et al. [29] found N_2-fixation one of the dominant processes in N-cycling occurring in deadwood, second only to the process of ammonia incorporation into organic molecules. On the other hand, the respiratory pathways utilizing nitrate or nitrite reduction (denitrification) appeared to be considerably less important in deadwood than in soil, while nitrification steps were

missing. Accordingly, we found the *nifH* gene the most abundant among the N-cycling genes quantified, followed by those related to denitrification (*nirK* and *nosZ*) and lastly *amoA* gene, related to the nitrification process. These findings are in contrast with soils where nitrification is the most widespread bacterial process within the N cycle [86].

We found a net N_2O consumption in all deadwood cores analysed except for one core of decay class 3. This finding suggests a complete denitrifying activity during our laboratory measurements. Similar results were obtained by Covey et al. [71]. Denitrifying bacteria are abundant and widespread in forest soils. Different enzymes (reductases) are sequentially involved in converting nitrate to N_2, passing through N_2O [87]. Not all denitrifiers harbour the complete battery of genes encoding all the denitrification reductases; some have truncated pathways. We found the highest values of *nirK* and *nosZ* genes copies number in late decay class 5, consistently with the highest values of N_2O consumption. It suggests that the highest abundance and diversity within the bacterial community could drive denitrification towards complete reduction of nitrate compounds, lowering N_2O.

The *amoA* gene, the key gene in the nitrification pathway, was only detected at low levels in both ammonia-oxidizing bacterial and archaeal communities. Ammonia oxidizers bacteria are also involved in N_2O emissions [88]. Little is known about the role of ammonia-oxidizing microorganisms in deadwood metabolic processes and although further analysis (such as transcripts detection or enzymatic activity) is required, their low abundance may suggest a relatively less involvement of this group of prokaryotes in N_2O fluxes from deadwood than denitrifying bacteria.

5. Conclusions

Due to the variety of measurements conducted, our mesocosm experiment provides significant insight into the microbial community patterns during deadwood decomposition. Dead black pine logs are proved to be an important habitat for fungi, bacteria, and archaea. These microbial communities were influenced by the chemical properties of the substrate, indicating that they are an active component of the wood-colonizing biota. Data obtained by real time PCR quantification were consistent with other findings attained by using other approaches such as next-generation sequencing (NGS) or metatranscriptomics, confirming that various bacterial groups act in wood decomposition. The highest abundance and microbial species diversity were revealed in the late decay classes with respect to the initial stages of decomposition. As decomposition progresses, the involvement of bacteria in wood decay appears to be increasingly crucial. In particular, our results lead to hypothesize complex adaptation of the bacterial community to changes in deadwood structure and composition, combining nutritional strategy with potential interaction with fungi.

The increasing number of bacterial and fungal species in the last decay classes evidenced by the present study is an important piece of information in developing forest strategies for deadwood management during silvicultural operations. In fact, harvesting operations can remove only logs of the first and second decay classes, while more decomposed logs must be left on soil surface because mechanical operations are impossible at this stage of decomposition. Forest managers must consider this aspect to maintain and improve biodiversity in managed and semi-natural forests. An amount of 20–50 m^3 ha^{-1} of logs should be preserved, adopting the principles of close-to-nature management. In the present case, the volume of logs is in this range. Preferably, this amount of deadwood should be spatially concentrated in a network of islands of senescence (1–2 hectares each) with an equal distribution by decay classes in each island of senescence.

Data obtained from laboratory measurements of gas fluxes reinforced the assumption of the strong involvement of deadwood microorganisms in GHG emissions in the forest ecosystem, adding awareness of the need for proper deadwood management in the context of climate change. Nevertheless, this aspect must be analysed and evaluated with an ecosystem service-balancing approach, considering the other important ecosystem services influenced by the presence of deadwood in the forest.

Supplementary Materials: The following are available online at https://www.mdpi.com/article/10.3390/f12101418/s1, Table S1: Description of visual characteristics used to assign the decay class. Table S2: Primer pairs used for real time PCR absolute quantification of the different microbial groups assessed in the five deadwood decay classes. Table S3: Maximum values of CO_2, CH_4, and N_2O production from black pine deadwood cores under laboratory experiment. Mean values according to each decay classes are also reported (standard errors in parentheses). Different letters in a column indicate significant differences at $p < 0.05$ (LSD test) among means. Table S4: ANOSIM and PERMANOVA global test based on the Bray–Curtis similarity matrices of 18S- and 16S-rDNA DGGE, for microbial groups (fungi, bacteria, and actinobacteria) decaying downy birch deadwood. Table S5: Values of ANOSIM statistic R (upper right side) and PERMANOVA statistic F (lower left side) from pairwise comparison of the banding profiles of fungal 18S-rDNA DGGE, and bacterial and actinobacterial 16S-rDNA DGGEs. Figure S1: Maximum values of CH_4 production (a) and archaeal methanogen 16S rDNA gene copies number (b) from each black pine deadwood sample. Figure S2: Maximum values of N_2O production (a) and *nir*K gene (b) and *nos*Z gene (c) copies number (botton) from each black pine deadwood sample. Figure S3: DGGE profiles of fungal 18S rDNA gene fragments (a), bacterial 16S rDNA gene fragments (b), and actinobacterial 16S rDNA gene fragments (c). The letter M on the gel images indicates the marker used for normalization of bands.

Author Contributions: Conceptualization, R.P. and I.D.M.; methodology, R.P., I.D.M., A.L. and A.P.; formal analysis, R.P. and A.E.A.; data curation, R.P., A.L.; writing—original draft preparation, R.P., I.D.M., A.L. and A.P. All authors have read and agreed to the published version of the manuscript.

Funding: This work was supported by the EU's LIFE+ "Nature and biodiversity" program through the SelPiBio LIFE project (Innovative silvicultural treatments to enhance soil biodiversity in artificial black pine stands, i.e., LIFE13 BIO/IT/000282) for demonstration of innovative silvicultural treatments in artificial black pine stands.

Institutional Review Board Statement: Not applicable.

Informed Consent Statement: Not applicable.

Data Availability Statement: The data presented in this study are available on request from the corresponding author.

Acknowledgments: The authors would like to thank Paolo Cantiani for financial support and the Coordination of the SelPiBio LIFE project. This paper is dedicated to the memory of Alessandro Elio Agnelli, our friend and colleagues, who left us too soon.

Conflicts of Interest: The authors declare no conflict of interest.

References

1. Humphrey, J.W.; Sippola, A.L.; Lempérière, G.; Dodelin, B.; Alexander, K.N.A.; Butler, J.E. Deadwood as an indicator of biodiversity in European forests: From theory to operational guidance. In *Monitoring and Indicators of Forest Biodiversity in Europe—From Ideas to Operationality*; Marchetti, M., Ed.; EFI Proceedings: Joensuu, Finland, 2004; Volume 51, pp. 193–206.
2. Müller, J.; Bütler, R. A Review of habitat thresholds for dead wood: A baseline for management recommendations in European forests. *Eur. J. For. Res.* **2010**, *129*, 981–992. [CrossRef]
3. Błońska, E.; Kacprzyk, M.; Spolnik, A. Effect of deadwood of different tree species in various stages of decomposition on biochemical soil properties and carbon storage. *Eco. Res.* **2017**, *32*, 193–203. [CrossRef]
4. Vallauri, D.; André, J.; Blondel, J. Deadwood—A typical shortcoming of Managed forests. *Rev. For. Française* **2003**, *2*, 99–112. (In French)
5. Herrero, C.; Monleon, V.J.; Gómez, N.; Bravo, F. Distribution of dead wood volume and mass in mediterranean *Fagus sylvatica* L. forests in Northern Iberian Peninsula. Implications for field sampling inventory. *For. Syst.* **2016**, *25*, e069. [CrossRef]
6. Ulyshen, M.D.; Hanula, J.L. Patterns of saproxylic beetle succession in loblolly pine. *Agric. For. Entomol.* **2010**, *12*, 187–194. [CrossRef]
7. Hammond, H.J.; Langor, D.W.; Spence, J.R. Saproxylic beetles (Coleoptera) using Populus in boreal aspen stands of western Canada: Spatiotemporal variation and conservation of assemblages. *Can. J. For. Res.* **2004**, *34*, 1–19. [CrossRef]
8. Næsset, E. Relationship between relative wood density of Picea abies logs and simple classification systems of decayed coarse woody debris. *Can. J. For. Res.* **1999**, *14*, 454–461. [CrossRef]
9. Paletto, A.; Tosi, V. Deadwood density variation with decay class in seven tree species of the Italian Alps. *Scand. J. For. Res.* **2010**, *25*, 164–173. [CrossRef]

10. IPCC. Guidelines for national greenhouse gas inventories, prepared by the National Greenhouse Gas Inventories Programme. In *Institute for Global Environmental Strategies (IGES)*; Eggelston, H.S., Buendia, L., Miwa, K., Ngara, T., Tanabe, K., Eds.; IPCC: Hayama, Japan, 2006.
11. Kahl, T.; Baber, K.; Otto, P.; Wirth, C.; Bauhus, J. Drivers of CO_2 emission rates from dead wood logs of 13 tree species in the initial decomposition phase. *Forests* **2015**, *6*, 2484–2504. [CrossRef]
12. Magnússon, R.Í.; Tietema, A.; Cornelissen, J.H.C.; Hefting, M.M.; Kalbitz, K. Tamm Review: Sequestration of carbon from coarse woody debris in forest soils. *For. Ecol. Manag.* **2016**, *377*, 1–15. [CrossRef]
13. Thomas, J. Dead wood: From forester's bane to environmental boon. In Proceedings of the Symposium on Ecology and Management of Deadwood in Western Forests; Laudenslayer, W.F.J., Shea, P.J., Valentine, B.E., Weatherspoon, C.P., Lisle, T.E., Eds.; Forest Service General Technical Report PSW-GTR-181. U.S. Forest Service: Reno, NV, USA, 2002; pp. 3–9.
14. Marage, D.; Lemperiere, G. The Management of snags: A comparison in Managed and unmanaged ancient forests of the Southern french Alps. *Ann. For. Sci.* **2005**, *62*, 135–142. [CrossRef]
15. Pelyukh, O.; Paletto, A.; Zahvoyska, L. People's attitudes towards deadwood in forest: Evidence from the Ukrainian Carpathians. *J. For. Sci.* **2019**, *65*, 171–182. [CrossRef]
16. Pommerening, A.; Murphy, S.T. A review of the history, definitions and methods of continuous cover forestry with special attention to afforestation and restocking. *Forestry* **2004**, *77*, 27–44. [CrossRef]
17. Dittrich, S.; Jacob, M.; Bade, C.; Leuschner, C.; Hauck, M. The significance of deadwood for total bryophyte, lichen, and vascular plant diversity in an old-growth spruce forest. *Plant Ecol.* **2014**, *215*, 1123–1137. [CrossRef]
18. Lee, M.R.; Oberle, B.; Olivas, W.; Young, D.F.; Zanne, A.E. Wood construction more strongly shapes deadwood microbial communities than spatial location over 5 years of decay. *Environ. Microb.* **2020**, *22*, 4702–4717. [CrossRef]
19. Alfaro, M.; Oguiza, J.A.; Ramírez, L.; Pisabarro, A.G. Comparative analysis of secretomes in basidiomycete fungi. *J. Proteomics* **2014**, *102*, 28–43. [CrossRef]
20. Johnston, S.R.; Boddy, L.; Weightman, A.J. Bacteria in decomposing wood and their interactions with wood-decay fungi. *FEMS Microbiol. Ecol.* **2016**, *92*, fiw179. [CrossRef]
21. Janusz, G.; Pawlik, A.; Sulej, J.; Świderska-Burek, U.; Jarosz-Wilkołazka, A.; Paszczyński, A. Lignin degradation: Microorganisms, enzymes involved, genomes analysis and evolution. *FEMS Microbiol. Rev.* **2017**, *41*, 941–962. [CrossRef]
22. Bani, A.; Pioli, S.; Ventura, M.; Panzacchi, P.; Borruso, L.; Tognetti, R.; Tonon, G.; Brusetti, L. The role of microbial community in the decomposition of leaf litter and deadwood. *Appl. Soil Ecol.* **2018**, *126*, 75–84. [CrossRef]
23. Wilhelm, R.C.; Singh, R.; Eltis, L.D.; Mohn, W.W. Bacterial contributions to delignification and lignocellulose degradation in forest soils with metagenomic and quantitative stable isotope probing. *ISME J.* **2019**, *13*, 413–429. [CrossRef]
24. Díaz-García, L.; Bugg, T.D.; Jiménez, D.J. Exploring the lignin catabolism potential of soil-derived lignocellulolytic microbial consortia by a gene-centric metagenomic approach. *Microb. Ecol.* **2020**, *80*, 885–896. [CrossRef]
25. Ho, A.; Angel, R.; Veraart, A.J.; Daebeler, A.; Jia, Z.; Kim, S.Y.; Kerckhof, F.M.; Boon, N.; Bodelier, P.L. Biotic interactions in microbial communities as modulators of biogeochemical processes: Methanotrophy as a model system. *Front. Microbiol.* **2016**, *7*, 1285. [CrossRef]
26. De Boer, W.; Van der Wal, A. Interactions between saprotrophic basidiomycetes and bacteria. In *Ecology of Saprotrophic Basidiomycetes*; Boddy, L., Frankland, J.C., van West, P., Eds.; Academic Press: Amsterdam, The Netherlands, 2008; pp. 143–153.
27. Clausen, C.A. Bacterial associations with decaying wood: A Review. *Int. Biodeterior. Biodegrad.* **1996**, *37*, 1–2. [CrossRef]
28. Rinne, K.T.; Rajala, T.; Peltoniemi, K.; Chen, J.; Smolander, A.; Mäkipää, R. Accumulation rates and sources of external nitrogen in decaying wood in a Norway spruce dominated forest. *Funct. Ecol.* **2017**, *31*, 530–541. [CrossRef]
29. Tláskal, V.; Brabcová, V.; Větrovský, T.; Jomura, M.; López-Mondéjar, R.; Monteiro, L.M.O.; Saraiva, J.P.; Human, Z.R.; Cajthaml, T.; da Rocha, U.N.; et al. Complementary roles of wood-inhabiting fungi and bacteria facilitate deadwood decomposition. *mSystems* **2021**, *6*, e01078–20. [CrossRef] [PubMed]
30. Lladó, S.; López-Mondéjar, R.; Baldrian, P. Forest soil bacteria: Diversity, involvement in ecosystem processes, and response to global change. *Microbiol. Mol. Biol. Rev.* **2017**, *81*, e00063–16.
31. Singh, B.K.; Bardgett, R.D.; Smith, P.; Reay, D.S. Microorganisms and climate change: Terrestrial feedbacks and mitigation options. *Nat. Rev. Microbiol.* **2010**, *8*, 779–790. [CrossRef] [PubMed]
32. Dahllöf, I. Molecular community analysis of microbial diversity. *Curr. Opin. Biotechnol.* **2002**, *13*, 213–217. [CrossRef]
33. Pastorelli, R.; Agnelli, A.E.; De Meo, I.; Graziani, A.; Paletto, A.; Lagomarsino, A. Analysis of microbial diversity and greenhouse gas production of decaying pine logs. *Forests* **2017**, *8*, 224. [CrossRef]
34. Pastorelli, R.; Paletto, A.; Agnelli, A.E.; Lagomarsino, A.; De Meo, I. Microbial communities associated with decomposing deadwood of downy birch in a natural forest in Khibiny Mountains (Kola Peninsula, Russian Federation). *For. Ecol. Manag.* **2020**, *455*, 117643. [CrossRef]
35. Pastorelli, R.; Costagli, V.; Forte, C.; Viti, C.; Rompato, B.; Nannini, G.; Certini, G. Litter decomposition: Little evidence of the "home-field advantage" in a mountain forest in Italy. *Soil Biol. Biochem.* **2021**, *159*, 108300. [CrossRef]
36. Lagomarsino, A.; Mazza, G.; Agnelli, A.E.; Lorenzetti, R.; Bartoli, C.; Viti, C.; Colombo, C.; Pastorelli, R. Litter fractions and dynamics in a degraded pine forest after thinning treatments. *Eur. J. For. Res.* **2020**, *139*, 295–310. [CrossRef]
37. Lagomarsino, A.; De Meo, I.; Agnelli, A.E.; Paletto, A.; Mazza, G.; Bianchetto, E.; Pastorelli, R. Decomposition of black pine (*Pinus nigra* JF Arnold) deadwood and its impact on forest soil components. *Sci. Total Environ.* **2021**, *754*, 142039. [CrossRef]

38. Petersen, D.G.; Blazewicz, S.J.; Firestone, M.; Herman, D.J.; Turetsky, M.; Waldrop, M. Abundance of microbial genes associated with nitrogen cycling as indices of biogeochemical process rates across a vegetation gradient in Alaska. *Environ. Microbiol.* **2012**, *14*, 993–1008. [CrossRef]
39. Rocca, J.D.; Lennon, J.T.; Evans, S.E. Relationships between protein-encoding gene abundance and corresponding process are commonly assumed yet rarely observed. *ISME J.* **2014**, *9*, 1693–1699. [CrossRef]
40. Lammel, D.R.; Feigl, B.J.; Cerri, C.C.; Nüsslein, K. Specific microbial gene abundances and soil parameters contribute to C.N. and greenhouse gas process rates after land use change in Southern Amazonian soils. *Front. Microb.* **2015**, *6*, 1057. [CrossRef]
41. Giuntini, F.; De Meo, I.; Graziani, A.; Cantiani, P.; Paletto, A. Stima del volume di legno morto in rimboschimenti di pino nero (*Pinus nigra* JF Arnold) in Toscana: Confronto tra casi studio. *Dendronatura* **2017**, *1*, 19–28. (In Italian)
42. Bayraktar, S.; Paletto, A.; Floris, A. Deadwood volume and quality in recreational forests: The case study of the Belgrade forest (Turkey). *For. Syst.* **2020**, *29*, e008.
43. Paletto, A.; Tosi, V. Forest canopy cover and canopy closure: Comparison of assessment techniques. *Eur. J. For. Res.* **2009**, *128*, 265–272. [CrossRef]
44. Cantiani, P.; De Meo, I.; Becagli, C.; Bianchetto, E.; Cazau, C.; Mocali, S.; Salerni, E. Effects of thinning on plants and fungi biodiversity in a *Pinus nigra* plantation: A case study in central Italy. *For. Ideas* **2015**, *21*, 149–162.
45. Barbato, D.; Perini, C.; Mocali, S.; Bacaro, G.; Tordoni, E.; Maccherini, S.; Marchi, M.; Cantiani, P.; De Meo, I.; Bianchetto, E.; et al. Teamwork makes the dream work: Disentangling cross-taxon congruence across soil biota in black pine plantations. *Sci. Total Environ.* **2019**, *656*, 659–669. [CrossRef]
46. Rivas-Martínez, S. Global Bioclimatics. (Clasificación Bioclimática de la Tierra). Available online: http://www.globalbioclimatics.org/book/bioc/global_bioclimatics_0.htm (accessed on 27 August 2004).
47. Vainio, E.J.; Hantula, J. Direct analysis of wood-inhabiting fungi using denaturing gradient gel electrophoresis of amplified ribosomal DNA. *Mycol. Res.* **2000**, *8*, 927–936. [CrossRef]
48. Nübel, U.; Engelen, B.; Felske, A.; Snaidr, J.; Wieshuber, A.; Amann, R.I.; Ludwig, W.; Backhaus, H. Sequence heterogeneities of genes encoding 16S rRNAs in *Paenibacillus polymyxa* detected by temperature gradient gel electrophoresis. *J. Bacteriol.* **1996**, *178*, 5636–5643. [CrossRef]
49. Heuer, H.; Krsek, M.; Baker, P.; Smalla, K.; Wellington, E.M.H. Analysis of actinomycetes communities by specific amplification of genes encoding 16S rRNA and gel-electrophoretic separation in denaturing gradients. *Appl. Environ. Microb.* **1997**, *63*, 3233–3241. [CrossRef]
50. Wang, J.; Yang, D.; Zhang, Y.; Shen, J.; van der Gast, C.; Hahn, M.W.; Wu, Q. Do patterns of bacterial diversity along salinity gradients differ from those observed for microorganisms? *PLoS ONE* **2011**, *6*, e27597.
51. Pastorelli, R.; Landi, S.; Trabelsi, D.; Piccolo, R.; Mengoni, A.; Bazzicalupo, M.; Pagliai, M. Effects of soil management on structure and activity of denitrifying bacterial communities. *Appl. Soil Ecol.* **2011**, *49*, 46–58. [CrossRef]
52. Hammer, Ø.; Harper, D.A.T.; Ryan, P.D. PAST: Paleontological statistics software package for education and data analysis. *Palaeontol. Electronica* **2001**, *4*, 9.
53. Ramette, A. Multivariate analyses in microbial ecology. *FEMS Microbiol. Ecol.* **2007**, *62*, 142–160. [CrossRef] [PubMed]
54. De Meo, I.; Lagomarsino, A.; Agnelli, A.E.; Paletto, A. Direct and indirect assessment of carbon stock in deadwood: Comparison in Calabrian Pine (*Pinus brutia* Ten. subsp. brutia) forests in Italy. *For. Sci.* **2019**, *65*, 460–468. [CrossRef]
55. Harmon, M.E.; Fasth, B.; Woodall, C.W.; Sexton, J. Carbon concentration of standing and downed woody detritus: Effects of tree taxa, decay class, position, and tissue type. *For. Ecol. Manag.* **2013**, *291*, 259–267. [CrossRef]
56. Weedon, J.T.; Cornwell, W.K.; Cornelissen, J.H.; Zanne, A.E.; Wirth, C.; Coomes, D.A. Global meta-analysis of wood decomposition rates: A role for trait variation among tree species? *Ecol. Lett.* **2009**, *12*, 45–56. [CrossRef]
57. Kahl, T.; Arnstadt, T.; Baber, K.; Bässler, C.; Bauhus, J.; Borken, W.; Buscot, F.; Floren, A.; Heibl, C.; Hessenmöller, D.; et al. Wood decay rates of 13 temperate tree species in relation to wood properties, enzyme activities and organismic diversities. *For. Ecol. Manag.* **2017**, *391*, 86–95. [CrossRef]
58. Palviainen, M.; Finér, L.; Laiho, R.; Shorohova, E.; Kapitsa, E.; Vanha-Majamaa, I. Carbon and nitrogen release from decomposing Scots pine, Norway spruce and silver birch stumps. *For. Ecol. Manag.* **2010**, *259*, 390–398. [CrossRef]
59. Lombardi, F.; Cherubini, P.; Tognetti, R.; Cocozza, C.; Lasserre, B.; Marchetti, M. Investigating biochemical processes to assess deadwood decay of beech and silver fir in Mediterranean mountain forests. *Ann. For. Sci.* **2013**, *70*, 101–111. [CrossRef]
60. Purahong, W.; Arnstadt, T.; Kahl, T.; Bauhus, J.; Kellner, H.; Hofrichter, M.; Krüger, D.; Buscot, F.; Hoppe, B. Are correlations between deadwood fungal community structure, wood physico-chemical properties and lignin-modifying enzymes stable across different geographical regions? *Fungal Ecol.* **2016**, *22*, 98–105. [CrossRef]
61. Cornelissen, J.H.C.; Sass-Klaassen, U.; Poorter, L.; van Geffen, K.; van Logtestijn, R.S.P.; van Hal, J.; Goudzwaard, L.; Sterck, F.J.; Klaassen, R.K.W.M.; Freschet, G.T.; et al. Controls on coarse wood decay in temperate tree species: Birth of the LOGLIFE Experiment. *AMBIO* **2012**, *1*, 231–245. [CrossRef]
62. Arnstadt, T.; Hoppe, B.; Kahl, T.; Kellner, H.; Krüger, D.; Bässler, C.; Bauhus, J.; Hofrichter, M. Patterns of laccase and peroxidases in coarse woody debris of *Fagus sylvatica, Picea abies* and *Pinus Sylvestris* and their relation to different wood parameters. *Eur. J. For. Res.* **2016**, *135*, 109–124. [CrossRef]
63. Salerni, E.; Barbato, D.; Cazau, C.; Gardin, L.; Henson, G.; Leonardi, P.; Tomao, A.; Perini, C. Selective thinning to enhance soil biodiversity in artificial black pine stands-what happens to mushroom fruiting? *Ann. For. Res.* **2020**, *63*, 75–90.

64. Hoppe, B.; Krüger, D.; Kahl, T.; Arnstadt, T.; Buscot, F.; Bauhus, J.; Wubet, T. A pyrosequencing insight into sprawling bacterial diversity and community dynamics in decaying deadwood logs of *Fagus sylvatica* and *Picea abies*. *Sci. Rep.* **2015**, *5*, 9456.
65. Zhang, H.B.; Yang, M.X.; Tu, R. Unexpectedly high bacterial diversity in decaying wood of a conifer as revealed by a molecular method. *Int. Biodeterior. Biodegrad.* **2008**, *62*, 471–474.
66. Větrovský, T.; Steffen, K.T.; Baldrian, P. Potential of cometabolic transformation of polysaccharides and lignin in lignocellulose by soil Actinobacteria. *PLoS ONE* **2014**, *9*, e89108. [CrossRef]
67. Rinta-Kanto, J.M.; Sinkko, H.; Rajala, T.; Al-Soud, W.A.; Sørensen, S.J.; Tamminen, M.V.; Timonen, S. Natural decay process affects the abundance and community structure of bacteria and archaea in *Picea abies* logs. *FEMS Microbiol. Ecol.* **2016**, *92*, fiw087. [CrossRef]
68. Gómez-Brandón, M.; Probst, M.; Siles, J.A.; Peintner, U.; Bardelli, T.; Egli, M.; Insam, H.; Ascher-Jenull, J. Fungal communities and their association with nitrogen-fixing bacteria affect early decomposition of Norway spruce deadwood. *Sci. Rep.* **2020**, *10*, 1–11.
69. Lynd, L.R.; Weimer, P.J.; van Zyl, W.H.; Pretorius, I.S. Microbial cellulose utilization: Fundamentals and biotechnology. *Microbiol. Mol. Biol. Rev.* **2020**, *66*, 506–577. [CrossRef]
70. Purahong, W.; Wubet, T.; Krüger, D.; Buscot, F. Molecular evidence strongly supports deadwood-inhabiting fungi exhibiting unexpected tree species preferences in temperate forests. *ISME J.* **2018**, *12*, 289–295. [CrossRef]
71. Covey, K.R.; de Mesquita, C.B.; Oberle, B.; Maynard, D.S.; Bettigole, C.; Crowther, T.W.; Duguid, M.C.; Steven, B.; Zanne, A.E.; Lapin, M.; et al. Greenhouse trace gases in deadwood. *Biogeochemistry* **2016**, *130*, 215–226. [CrossRef]
72. Carmichael, M.J.; Bernhardt, E.S.; Bräuer, S.L.; Smith, W.K. The role of vegetation in methane flux to the atmosphere: Should vegetation be included as a distinct category in the global methane budget? *Biogeochemistry* **2014**, *119*, 1–24. [CrossRef]
73. Lenhart, K.; Bunge, M.; Ratering, S.; Neu, T.R.; Schüttmann, I.; Greule, M.; Kammann, C.; Schnell, S.; Müller, C.; Zorn, H.; et al. Evidence for methane production by saprotrophic fungi. *Nat. Commun.* **2012**, *3*, 1–8. [CrossRef] [PubMed]
74. Zeikus, J.G.; Henning, D.L. Methanobacterium arbophilicum sp. nov. An obligate anaerobe isolated from wetwood if living trees. *Anton. Leeuw.* **1975**, *41*, 543–552. [CrossRef] [PubMed]
75. Mukhin, V.A.; Voronin, P.Y. A new source of methane in boreal forests. *Appl. Biochem. Microbiol.* **2008**, *44*, 297–299. [CrossRef]
76. Beckmann, S.; Krueger, M.; Engelen, B.; Gorbushina, A.A.; Cypionka, H. Role of bacteria, archaea and fungi involved in methane release in abandoned coal mines. *Geomicrobiol. J.* **2011**, *28*, 347–358. [CrossRef]
77. Moll, J.; Keller, H.; Leonhardt, S.; Stengel, E.; Dahl, A.; Bässler, C.; Buscot, F.; Hofrichter, M.; Hoppe, B. Bacteria inhabiting deadwood of 13 tree species are heterogeneously distributed between sapwood and heartwood. *Environ. Microbiol.* **2018**, *20*, 3744–3756. [CrossRef] [PubMed]
78. Kudo, T. Termite-microbe symbiotic system and its efficient degradation of lignocellulose. *Biosci. Biotechnol. Biochem.* **2009**, *73*, 2561–2567. [CrossRef] [PubMed]
79. Hongoh, Y.; Ohkuma, M. Termite gut flagellates and their methanogenic and eubacterial symbionts. In *Endosymbiotic Methanogenic Archaea*; Hackstein, J.H.P., Ed.; Springer: Berlin/Heidelberg, Germany, 2010; Volume 19, pp. 55–79.
80. Hirakata, Y.; Hatamoto, M.; Oshiki, M.; Watari, T.; Araki, N.; Yamaguchi, T. Food selectivity of anaerobic protists and direct evidence for methane production using carbon from prey bacteria by endosymbiotic methanogen. *ISME J.* **2020**, *14*, 1873–1885. [CrossRef]
81. Folman, L.B.; Gunnewiek, P.; Boddy, L.; De Boer, W. Impact of white-rot fungi on numbers and community composition of bacteria colonizing beech wood from forest soil. *FEMS Microbiol. Ecol.* **2008**, *63*, 181–191. [CrossRef]
82. Vorob'ev, A.V.; de Boer, W.; Folman, L.B.; Bodelier, P.L.; Doronina, N.V.; Suzina, N.E.; Trotsenko, Y.A.; Dedysh, S.N. *Methylovirgula ligni* gen. nov., sp. nov., an obligately acidophilic, facultatively methylotrophic bacterium with a highly divergent *mxa*F gene. *Int. J. Syst. Evol. Microbiol.* **2009**, *59*, 2538–2545. [CrossRef]
83. Mäkipää, R.; Leppänen, S.M.; Munoz, S.S.; Smolander, A.; Tiirola, M.; Tuomivirta, T.; Fritze, H. Methanotrophs are core members of the diazotroph community in decaying Norway spruce logs. *Soil Biol. Biochem.* **2018**, *120*, 230–232. [CrossRef]
84. Dedysh, S.N.; Khmelenina, V.N.; Suzina, N.E.; Trotsenko, Y.A.; Semrau, J.D.; Liesack, W.; Tiedje, J.M. *Methylocapsa acidiphila* gen. nov., sp. nov., a novel methane-oxidizing and dinitrogen-fixing acidophilic bacterium from Sphagnum bog. *Int. J. Syst. Evol. Microbiol.* **2002**, *52*, 251–261. [CrossRef]
85. Wagg, C.; Schaeppi, K.; Banerjee, S.; Kuramae, E.E.; van der Heijden, M.G.A. Fungal-bacterial diversity and microbiome complexity predict ecosystem functioning. *Nat. Commun.* **2019**, *10*, 1–10.
86. Žifčáková, L.; Větrovský, T.; Lombard, V.; Henrissat, B.; Howe, A.; Baldrian, P. Feed in summer, rest in winter: Microbial carbon utilization in forest topsoil. *Microbiome* **2017**, *5*, 122. [CrossRef] [PubMed]
87. Zumft, W.G. Cell biology and molecular basis of denitrification. *Microbiol. Mol. Biol. Rev.* **1997**, *61*, 533–616. [CrossRef]
88. Shaw, L.J.; Nicol, G.W.; Smith, Z.; Fear, J.; Prosser, J.I.; Baggs, E.M. *Nitrosospira* spp. can produce nitrous oxide via a nitrifier denitrification pathway. *Environ. Microbiol.* **2006**, *8*, 214–222. [CrossRef]